

This document is confidential and is proprietary to the American Chemical Society and its authors. Do not copy or disclose without written permission. If you have received this item in error, notify the sender and delete all copies.

Consumption of a natural high intensity sweetener enhances activity and expression of rabbit intestinal Na⁺/glucose cotransporter 1 (SGLT1) and improves colibacillosis- induced enteric disorders.

Journal:	<i>Journal of Agricultural and Food Chemistry</i>
Manuscript ID	jf-2019-04995u.R1
Manuscript Type:	Article
Date Submitted by the Author:	03-Oct-2019
Complete List of Authors:	Moran, Andrew; University of Liverpool Faculty of Health and Life Sciences, Institute of Integrative Biology Al-Rammahi, Miran; University of Liverpool Faculty of Health and Life Sciences, Functional & Comparative Genomics Daly, Kristian; University of Liverpool Faculty of Health and Life Sciences, Institute of Integrative Biology Grand, Emeline; Neovia SAS Ionescu, Catherine ; Pancosma SA Bravo, David; Pancosma SA Wall, Emma; Pancosma SA Shirazi-Beechey, Soraya P.; University of Liverpool Faculty of Health and Life Sciences, Institute of Integrative Biology

SCHOLARONE™
Manuscripts

1 **Consumption of a natural high intensity sweetener enhances activity and expression of**
2 **rabbit intestinal Na⁺/glucose cotransporter 1 (SGLT1) and improves colibacillosis-**
3 **induced enteric disorders.**

4 Andrew W. Moran^{†,1}, Miran A. Al-Rammahi^{†,‡,1}, Kristian Daly[†], Emeline Grand[§], Catherine
5 Ionescu^{||}, David M. Bravo^{||,1}, Emma H. Wall^{||,2}, and Soraya P. Shirazi-Beechey^{*,†}

6

7 [†]Epithelial Function and Development Group, Institute of Integrative Biology, University of
8 Liverpool, Liverpool L69 7ZB, United Kingdom

9 [‡]Zoonotic Disease Research Unit, College of Veterinary Medicine, University of Al-
10 Qadisiyah, Al-Diwaniyah, Iraq

11 [§] Neovia, Saint Nolff, France

12 ^{||} Pancosma SA, Geneva, Switzerland

13

14 ¹Current affiliation: Land O' Lakes, Minneapolis, Minnesota

15 ²Current affiliation: Erbo Group, Buetzberg, Switzerland

16 Corresponding author: Tel: +44 (0)151 794 4255, spsb@liverpool.ac.uk

17

18 **Running title:** Natural sweetener improves enteric disorders.

19

20

21

22

23 **ABSTRACT**

24 Absorption of glucose, via intestinal Na⁺/glucose cotransporter 1 (SGLT1), activates salt and
25 water absorption and is an effective route for treating *Escherichia coli* (*E. coli*)-induced
26 diarrhea. Activity and expression of SGLT1 is regulated by sensing of sugars and
27 artificial/natural sweeteners by the intestinal sweet receptor, T1R2-T1R3 expressed in
28 enteroendocrine cells. Diarrhea, caused by the bacterial pathogen *E-coli* is the most common
29 post-weaning clinical feature in rabbits, leading to mortality. We demonstrate here, that in
30 rabbits with experimentally *E-coli* - induced diarrhea, inclusion of a supplement containing
31 stevia leaf extract (SL) in the feed improves clinical signs of disease. We show that the rabbit
32 intestine expresses T1R2-T1R3. Furthermore, intake of SL enhances activity and expression
33 of SGLT1, and the capacity to absorb glucose. Thus, a natural plant extract sweetener can act
34 as an effective feed additive for lessening the negative impact of enteric disease in animals.

35

36 Key words: Colibacillosis; Oral rehydration; Rabbit; SGLT1; Intestinal T1R2-T1R3

37

38

39 INTRODUCTION

40 Na⁺/glucose co-transporter 1, SGLT1, is the major route for absorption of glucose across the
41 intestinal brush border membrane. Absorption of glucose via SGLT1 activates electrolyte and
42 water absorption. In humans, this strategy has been used in oral rehydration therapy, which is
43 the safest and most effective remedy for treating life-threatening diarrhea induced by agents
44 such as *Vibrio cholerae* and *Escherichia coli*.^{1,2} The condition is caused by toxic peptides
45 produced by bacteria stimulating the conversion of guanosine 5'-triphosphate (GTP) to cyclic
46 guanosine 5'-monophosphate (cGMP) by the enzyme guanylate cyclase. Increased
47 intracellular cGMP inhibits intestinal fluid uptake, resulting in net fluid secretion and thus
48 diarrhea.

49 The gut epithelium can sense sugars and artificial sweeteners via the sweet receptor
50 comprising of Taste family 1 Receptor 2 (T1R2) and 3 (T1R3) expressed on the luminal
51 membrane of enteroendocrine cells (EEC).^{3,4} This results in secretion of gut hormones,
52 glucagon-like peptide 1 (GLP-1), glucagon-like peptide 2 (GLP-2) and glucose-dependent
53 insulinotropic peptide (GIP) from EEC.^{5,6} GLP-2 upregulates SGLT1 activity and
54 expression^{7,8} in neighboring absorptive enterocytes via a neuro-paracrine pathway.^{6,9} GLP-2
55 also increases villus height and intestinal barrier function^{10,11}, thereby promoting gut health.
56 These effects have also been reported in piglets;¹² calves and ruminants.¹³

57 The sweet taste receptor is similarly activated by natural, high-intensity sweeteners, such as
58 stevia¹⁴ leading to increased expression and activity of SGLT1, providing the capacity for
59 enhanced glucose (electrolyte and water) absorption.

60 Rabbits are raised for a variety of commercial reasons. Their meat, wool and fur are valuable
61 commodities, as is their nitrogen-rich manure and high protein milk. They are also very
62 popular as household pets. Diarrhea is the most common post-weaning clinical feature in
63 rabbits, leading to significant rates of mortality. With current trends aimed at decreasing the

64 use of antibiotics, feed additives that can improve rabbit health and performance in the face
65 of disease is highly desirable. This is especially relevant in Europe, where antibiotic use in
66 animal feed is already banned, and the use of natural alternatives, for disease prevention, is
67 encouraged. Furthermore, in Europe the use of artificial sweeteners, used routinely in farm
68 animal nutrition,^{12,13} is prohibited as supplements in rabbit feed. It is not known if a natural
69 high-intensity sweetener such as stevia leaf extract (**SL**), which can be used in rabbit feed,
70 will elicit similar effects as seen with artificial sweeteners in farm animals, assisting to
71 prevent and ameliorate enteric diseases in rabbits.

72 Here we show that when rabbits are challenged with colibacillosis, inclusion of a supplement
73 containing SL in rabbit feed leads to significant reduction in diarrhea and bloat, improved
74 health, and decreased mortality. Furthermore, we demonstrate that rabbit intestine expresses
75 the intestinal sweet receptor T1R2-T1R3, and that inclusion of SL in the feed results in
76 upregulation of SGLT1 activity, protein and mRNA abundance in the small intestine. Thus, a
77 better understanding of the molecular mechanism underlying intestinal nutrient absorption
78 provides a rational strategy for using a natural feed additive for alleviating enteric disorders
79 and promoting health and well-being of animals.

80

81 MATERIALS AND METHODS

82 Chemicals

83 SL supplement (containing 25% stevia leaf extract and 2% *capsicum oleoresin* (for
84 concentration see below); TakTik Rabbit), was from Pancosma, Geneva, Switzerland. Zymo
85 Total RNA isolation kit with on-column DNase 1 digestion, was from Cambridge Bioscience,
86 Cambridge, UK. dT₂₀ primers and superscript III reverse transcriptase was from Life
87 Technologies, Paisley, UK and QIAquick PCR purification kit from Qiagen, Crawley, West
88 Sussex, UK. Consensus primers for mammalian T1R2 and T1R3 were purchased from
89 Eurogentec, Seraing, Belgium. Q5 Hot Start High-Fidelity DNA Polymerase was purchased
90 from New England Biolabs, Hitchin, Herts, UK, and pGEM-T Easy vector from Promega,
91 Southampton, UK. SYBR green JumpStart *Taq* ReadyMix, dithiothreitol, benzamidine,
92 phenolmethylsulfonyl fluoride, Bio-Max Light Chemiluminescence Film, β -actin antibody
93 (clone AC-15), D.P.X. neutral mounting medium, donkey serum, 10% neutral buffered
94 formalin and Mayer's Haemalum (3.3 mmol/L Mayer's Haemalum-haematoxylin, 1 mmol/L
95 sodium iodate, 0.42 mmol/L potassium alum) were purchased from Sigma-Aldrich, Poole,
96 Dorset, UK. Bio-Rad protein assay solution and polyvinylidene difluoride (PVDF) membrane
97 were from Bio-Rad Laboratories Ltd. Hemel Hempstead, UK. The antibody to SGLT1 was
98 raised in rabbits (custom synthesis) to a recombinant peptide corresponding to amino acids
99 554-640 of rabbit SGLT1 protein. Horseradish peroxidase-linked secondary antibodies were
100 purchased from DAKO Ltd, Cambridge, UK. Immobilon Western Chemiluminescent HRP
101 Substrate and cellulose acetate/nitrate filter were purchased from Millipore, Hertfordshire,
102 UK and [U-¹⁴C]-D-glucose (10.6 GBq/mmol) from Perkin Elmer, Seer Green, Bucks, UK.
103 Scintillation fluid (Optiphase HiSafe 3), was purchased from Fisher Scientific, UK and Eosin
104 Y solution (1 % [w/v] eosin aqueous) was from HD Supplies, Buckingham, Bucks, UK.
105 Chromogranin A antibody was from Abcam, Cambridge, UK. Antibodies to T1R2 and T1R3

106 are from Santa Cruz Biotechnology, INC., Heidelberg, Germany, and IgG Cy3- FITC-
107 conjugated secondary antibodies from Stratech Scientific, Newmarket, UK. 4',6-diaminido-2-
108 phenylindole (DAPI) was purchased from Vector Laboratories, Peterborough, UK.

109

110 **Phase 1:**

111 **Animals, Treatments and Experimental condition.** The animal experiment was conducted
112 at the Talhouet Research Center (Saint Nolf, France). All animal procedures were approved
113 by the Ethical Committee for Animal Experimentation of NEOVIA and by the Ministry of
114 Higher Education, of Research and Innovation, France (experimental reference # 03835.03).
115 Animal numbers were determined based on power calculations conducted using data from
116 previous experiments performed in the same facility wherein colibacillosis challenge was
117 used. Thirty-six day old Souche Hyplus PS59 rabbits (<http://www.hypharm.fr>; n = 300) were
118 weaned, blocked by sex, litter origin and body weight, and assigned to one of four dietary
119 treatments (n = 75/trt): un-supplemented diet or a diet supplemented with 50, 75, or 100 ppm
120 of SL, containing a maximum of 3.3, 4.9 and 6.5 μ M capsaicin). Animals were housed in
121 cages (5 rabbits per cage) with *ad libitum* access to feed and water. Rabbit feed was
122 formulated for a typical fattening ration containing 15.5% crude protein and ME of 22.9
123 kcal/100 g feed. All feed was free of antibiotics and medications, including coccidiostats.
124 The room was maintained at 19°C and was illuminated between 0700 and 1700 each day. All
125 animals were monitored daily.

126 On day 44 of age (day 0 of infection), all rabbits were orally inoculated with 5×10^6 CFU/mL
127 of *E. Coli* O103 LY265 inoculum (INRA, Nouzilly, France; dose determined in preliminary
128 experiments and validated in several separate experiments).

129

130 **Measurements.** Feed intake was measured daily per cage by weighing of refusals. Live
131 weights of individual rabbits were measured on days -2, 5, 12, 19 and 26 post infection
132 (corresponding to 42, 49, 56, 63, 70 d of age), and average daily gain (ADG) was calculated
133 from individual body weights. Feed efficiency (G:F; gain/feed) was calculated per cage.
134 Morbidities [visual signs of diarrhea and discoloration of feces, bloat (swollen stomach, dull
135 fur, low energy), and mobility] were assessed daily by two technicians trained by a
136 veterinarian. Morbidities were not quantified but were simply noted as present or absent
137 based on subjective visual observation by both technicians. The same technicians performed
138 the scoring throughout the study to avoid variation due to observer. Mortalities were also
139 recorded daily; dead animals were removed from cages upon detection and visible clinical
140 signs were noted. At the peak of mortality during clinical disease, a random selection of
141 rabbits (n = 10) was necropsied to verify colibacillosis as the cause of death (via *E. coli*
142 serotyping of intestinal content).

143 The experiment ended on day 26 post infection (when animals were 70 d of age) and all
144 remaining animals were euthanized by a trained technician. Average body weight at 70 d of
145 age was multiplied by the number of animals alive to estimate production weight per
146 treatment.

147

148 **Statistical Analysis.** Data were analyzed by ANOVA using the SAS Mixed Procedure with a
149 Dunnett's adjustment for multiple comparisons and orthogonal contrasts to test for linearity.
150 Treatment and time were fixed effects whereas sex and cage were treated as random effects.
151 Statistical significance was set at $p < 0.05$.

152

153 **Phase 2:**

154 The experiments in Phase 2 were undertaken to understand the molecular mechanisms
155 underlying the intestinal response of rabbits to SL.

156 **Animals, dietary trial, gut tissue sampling.** The animal experiment was conducted at the
157 Talhouet Research Center (Saint Nolff, France). All animal procedures were approved by the
158 Ethical Committee for Animal Experimentation of NEOVIA and by the Ministry of Higher
159 Education, of Research and Innovation, France (experimental reference # 03835.03). Animal
160 numbers were determined using gut responses and variation associated with supplementation
161 with artificial sweetener reported in published articles.^{6,12,13} Forty-two 60-day-old Souche
162 Hyplus PS59 rabbits (<http://www.hypharm.fr>) were blocked by sex and body weight and
163 assigned to one of two dietary treatments starting on day 61 of age (n = 21 rabbits/treatment):
164 un-supplemented diet or a diet supplemented with 75 ppm SL (dose chosen based on
165 responses observed in Phase 1). Animals were housed in cages (5 rabbits per cage) with *ad*
166 *libitum* access to feed and water. Rabbit feed was formulated for a typical fattening ration
167 containing 15.5% crude protein and ME of 22.9 kcal/100 g feed. All feed was free of
168 antibiotics and medications, including coccidiostats. The room was maintained at 19°C and
169 was illuminated between 0700 and 1700 each day. After the 9-day treatment period (the
170 period of 9 days was selected to cover the gut epithelial cell turnover that takes 4-5 days in
171 the majority of species and was extended to 9 days due to travel delays for the researcher
172 from the UK travelling to France for harvesting intestinal tissues) at 70 days of age (same
173 slaughter age as phase 1), all rabbits were weighed and euthanized by intra-cardiac injection
174 of Euthasol[®] after sedation starting at 9am. Intestinal tissues were removed, duodenal: 10 cm
175 distal to the pyloric caeca, ileal: 10 cm proximal from the ileocecal valve, jejunal; at the mid-
176 point between the pyloric caeca and ileocecal valve. Tissue samples collected from 10
177 rabbits/treatment (blocked by sex and body weight at slaughter), rinsed in ice cold saline and
178 either placed into cryovials or wrapped in aluminum foil and frozen immediately in liquid

179 nitrogen or pinned to dental plastic and fixed in 10% neutral buffered formalin at 4°C. Fixed
180 tissues were transferred to 20% sucrose in PBS after 24 h and stored at 4°C. Frozen tissues
181 were stored at -80°C before shipping to the UK on dry ice, whilst fixed samples were shipped
182 to the UK on wet ice, for subsequent analysis.

183

184 **Cloning of rabbit T1R2 and T1R3.** Total RNA was isolated from rabbit intestinal tissues
185 using the Zymo Total RNA isolation kit with on-column DNase 1 digestion. RNA was
186 quantified by UV spectrophotometry (assuming an OD₂₆₀ value of 1 = 40 µg/mL) and
187 integrity determined by agarose gel electrophoresis. Complementary DNA (cDNA) was
188 prepared using oligo dT₂₀ primers and superscript III reverse transcriptase, purified using
189 QIAquick PCR purification kit and quantified by UV spectrophotometry (assuming an OD₂₆₀
190 value of 1 = 33 µg/mL). Consensus primers for mammalian T1R2 and T1R3 are listed in
191 Table 1. Each PCR reaction mix contained 0.5 µmol/L of each forward and reverse primer,
192 0.5 U of Q5 Hot Start High-Fidelity DNA Polymerase, and 25 ng template cDNA in a final
193 volume of 25 µl. PCR cycling was carried out as follows: initial denaturation at 98°C for 1
194 min, 25 cycles of denaturation at 98°C for 10 s, annealing for 10 s and extension at 72°C for
195 30 s, followed by a final extension step at 72°C for 2 min. PCR amplicons were gel purified
196 using 1% agarose gels, cloned into pGEM-T Easy vector and custom sequenced (Eurofins-
197 MWG, Ebersberg, Germany). Sequence alignments and amino acid translations were
198 performed using commercial software (Vector NTI, Life Technologies).

199 The radial phylogram shown in Figure 7, depicting the phylogenetic relationship of rabbit
200 T1R3 to various mammalian homologs, was constructed by neighbor-joining analysis¹⁵ of
201 distance matrices generated using the PROTDIST program (Jones-Taylor-Thornton similarity
202 model),¹⁶ as part of the phylogenetic inference package, PHYLIP.¹⁷

203

204 **Table 1.** Primers used for PCR and qPCR.

Primer name	Accession No.	sequence	T _m / °C
RbACTB S	NM_001101683	5'-CCTTCTACAACGAGCTGCGAG-3'	51.4
RbACTB AS	NM_001101683	5'-GCCCTCGTAGATGGGTACTG-3'	49.9
RbPOLR2A S	XM_017348893.1	5'-ACGCTGCTCTTCAACATCCA-3'	60
RbPOLR2A AS	XM_017348893.1	5'-CCAGCGTAGTGGAAGGTGTT-3'	60
RbB2M S	XM_008269078.2	CTAGTCTTGTTCCCCTGCCT	58.9
RbB2M AS	XM_008269078.2	ATCAATCTGGGGCGGATGAAA	60
RbT1R2 S	XM_017346518	5'-TCTGGAACGTCAGCTTCACC-3'	52.5
RbT1R2 AS	XM_017346518	5'-GTGCTTCAGCATGGGGTAGT-3'	51.6
RbT1R3 S		5'-GCAAGTTCTTCAGCTTCTTCCT-3'	51.5
RbT1R3 AS		5'-TACATGTTCTCCAGGAGCTGC-3'	51.9
RbSGLT1 S	NM_001101692	5'-TGTC AAGGCTGGCTGTATCC-3'	51.4
RbSGLT1 AS	NM_001101692	5'-CTCCTCTGGTTCCACGCAA-3'	51.3

205

206 **Quantitative PCR.** Relative mRNA expression in the intestine was determined by
207 quantitative real-time PCR (qPCR). cDNA was prepared from total RNA as described above
208 and diluted to 5 ng/μL. Primers to rabbit SGLT1, β-actin (ACTB), RNA polymerase II
209 (POLR2A), and β-2-microglobulin (B2M) were designed using Primer-BLAST¹⁸ and
210 purchased from Eurogentec (see Table 1). Each qPCR reaction consisted of 25 ng cDNA
211 template, 1 X SYBR green JumpStart *Taq* ReadyMix and 900 nmol/L of each primer in a
212 total volume of 25 μL. The PCR cycling consisted of initial denaturation at 95°C for 2 min
213 followed by 45 cycles of 95°C for 15 s and 60°C for 1 min. Assays were performed in
214 triplicate using a RotorGene 3000 (Qiagen) with relative abundance calculated using RG-
215 3000 comparative quantification software (Qiagen). Abundance of SGLT1 mRNA was
216 normalized to the genomic mean of ACTB, POLR2A and B2M housekeeping genes, the
217 expression of which did not change throughout the study. qPCR assays without the RT step
218 were routinely employed as negative controls and showed no amplification. Melt curve

219 analysis showed no primer dimer formation in the assays. PCR amplicons were cloned into
220 pGEM-T easy vectors and sequenced to confirm veracity.

221

222 **Preparation of Brush Border Membrane Vesicles.** Brush border membrane vesicles

223 (BBMV) were isolated from different regions of rabbit small intestinal tissues based on the

224 procedure described by Shirazi-Beechey et al.,¹⁹ with modifications outlined by Rowell-

225 Schäfer et al.²⁰ and Dyer et al.²¹ All steps were carried out at 4°C. Tissues were thawed in a

226 buffer solution (100 mmol/L mannitol, 2 mmol/L HEPES/Tris pH 7.1 with protease

227 inhibitors, 0.5 mmol/L dithiothreitol, 0.2 mmol/L benzamidine, and 0.2 mmol/L

228 phenolmethylsulfonyl fluoride), cut into small pieces and vibrated for 1.5 min at speed 5

229 using a FUNDAMIX vibro-mixer (DrM, Dr Mueller AG, Maennedorf, Switzerland), in order

230 to free intestinal epithelial cells. The filtrate was then homogenized using a Polytron (Ystral,

231 Reading, Berkshire, UK) for 20 s. Next, MgCl₂ was added to a final concentration of 10

232 mmol/L and the solution stirred on ice for 20 min. The suspension was then centrifuged for

233 10 min at 3,000 x g (SS34 rotor, Sorvall, UK) and the resulting supernatant was spun for 30

234 min at 30,000 x g. The pellet was suspended in buffer (100 mmol/L mannitol, 0.1 mmol/L

235 MgSO₄, and 20 mmol/L HEPES/Tris pH 7.1) and homogenized with 10 strokes of a Potter

236 Elvehjem Teflon hand-held homogenizer before centrifuging for 30 min at 30,000 x g. The

237 final pellet was re-suspended in an isotonic buffer solution (300 mmol/L mannitol, 0.1

238 mmol/L MgSO₄, and 20 mmol/L HEPES/Tris pH 7.4) and homogenized by passing through a

239 27-gauge needle several times. The protein concentration in the BBMV was estimated by its

240 ability to bind Coomassie blue according to the Bio-Rad assay technique. Porcine γ -globulin

241 was used as the standard. Inclusion of protease inhibitors in the buffers is essential for

242 avoiding SGLT1 protein degradation.

243 In preparation for western blot analysis, aliquots of freshly prepared BBMV were diluted
244 with sample buffer (62.5 mmol/L Tris/HCl pH 6.8, 10% [v/v] glycerol, 2% [w/v] SDS, 0.05%
245 [v/v] β -mercaptoethanol, 0.05% [w/v] bromophenol blue) and stored at -20°C until use. The
246 remaining BBMV were divided into aliquots and stored in liquid nitrogen or used
247 immediately for glucose uptake studies.

248

249 **Western Blotting.** The abundance of SGLT1 and β -actin proteins in the BBMV isolated
250 from rabbit small intestine was determined by western blotting as described previously.^{12,21}
251 Protein components of BBMV (20 μ g) were separated by sodium dodecyl sulfate (SDS)-
252 polyacrylamide gel electrophoresis on 8% (w/v) polyacrylamide mini gels, containing 0.1%
253 (w/v) SDS, and electrotransferred to polyvinylidene difluoride (PVDF) membrane. The
254 PVDF membranes were blocked for 1 h at RT in PBS containing 0.5% (w/v) non-fat dried
255 milk, and 0.05% (v/v) Tween-20 (PBS-TM). Incubation for 1 hour with the SGLT1 antibody
256 diluted 1:1,000 in PBS-TM then followed.
257 Immuno-reactive bands were detected by incubation for 1 h with affinity purified horseradish
258 peroxidase-linked anti-rabbit secondary antibody diluted 1:2,000 in PBS-TM, and visualized
259 using Immobilon Western Chemiluminescent HRP Substrate and Bio-Max Light
260 Chemiluminescence Film. The intensity of the immunoreactive bands was quantified using
261 scanning densitometry (Total Lab, Newcastle-upon-Tyne, UK).
262 The PVDF membranes were stripped by 3 x 10 min washes in 137 mmol/L NaCl, 20 mmol/L
263 glycine/HCl (pH 2.5) and then re-probed with a monoclonal antibody to β -actin used as a
264 loading control. Blocking solution consisted of 0.1% (v/v) Triton X-100 and 0.1 mmol/L
265 EDTA in PBS (PBS-TE) and 5% (w/v) skimmed milk powder. PBS-TE was used for the
266 incubation and washing buffers. Horseradish peroxidase-linked anti-mouse secondary
267 antibody diluted 1:2,000 in PBS-TE was used, and visualized as above.

268

269 **Measurement of Na⁺-dependent glucose uptake.** Na⁺-dependent glucose uptake into rabbit
270 intestinal BBMV was measured as described.^{12,19} The uptake of D-glucose was initiated by
271 the addition of 100 μ L of incubation medium (100 mmol/L NaSCN [or KSCN], 100 mmol/L
272 mannitol, 20 mmol/L HEPES/Tris [pH 7.4], 0.1 mmol/L MgSO₄, 0.02% [w/v] NaN₃ and 0.1
273 mmol/L [U-¹⁴C]-D-glucose [10.6 GBq/mmol,]) to BBMV (100 μ g protein) at 37°C. The
274 reaction was stopped after 3 s by the addition of 1 mL of ice-cold stop buffer (150 mmol/L
275 KCl 20 mmol/L HEPES/Tris [pH 7.4], 0.1 mmol/L MgSO₄, 0.02% [w/v] NaN₃ and 0.1
276 mmol/L phlorizin). Aliquots (0.9 mL) of the reaction mixture were removed and filtered
277 under vacuum through a 0.22 μ m pore cellulose acetate/nitrate filter. The filter was washed
278 with 5 x 1 mL of ice-cold stop buffer, placed in a vial containing 4 mL of scintillation fluid
279 and the radioactivity retained on the filter measured using a Tri-Carb 2910TR Liquid
280 Scintillation Analyzer (PerkinElmer, Bucks, UK). All uptakes were measured in duplicate.

281

282 **Morphometry.** Rabbit small intestinal tissue was fixed and cryo-protected before embedded
283 in OCT (Fisher Scientific, UK), frozen at -20°C and then kept at -80°C until use. Tissue
284 blocks were sectioned (10 μ m) on a cryostat (Leica, CM 1900UV-1-1, Milton Keynes,
285 Buckinghamshire, UK) and thaw-mounted onto polylysine-coated slides. Morphometric
286 analysis was performed as described previously.¹² The sections were exposed to tap water for
287 1 min, transferred to Mayer's Haemalum for 1 min and washed gently with running tap water
288 for 5 min. They were stained with eosin Y solution for 30 s and subsequently dehydrated by
289 stepwise washing in 70% ethanol (v/v) for 2 x 1-min, absolute ethanol for 2 x 1-min, and
290 xylene for 3 x 1-min, before mounting with D.P.X. neutral mounting medium.
291 Digital images were captured with an Eclipse E400 microscope and DXM 1200 digital
292 camera (Nikon, Kingston upon Thames, Surrey, UK), analyzed using ImageJ software

293 (Wayne Rasband, US National Institutes of Health, Bethesda, MD) and calibrated using a 100
294 μm gradient slide. The crypt depth and the villus height were measured as the average
295 distance from crypt base to crypt-villus junction and villus base to villus tip, respectively. The
296 villus height and the crypt depth measurements were taken from an average of sixteen well
297 oriented crypt-villus units. A minimum of three images were captured per section with a
298 minimum of 8 sections prepared per animal, with each section being 5 sections apart within
299 the block. All images were captured under the same conditions with care taken to ensure that
300 the same villus was not counted twice.

301

302 **Immunohistochemistry.** Immunohistochemistry was performed as previously described.²²
303 Tissue sections (10 μm thick, on polylysine coated slides) were washed five times for 5 minutes
304 each in PBS. Slides were then incubated for 1 hour in blocking solution (10% (v/v) donkey
305 serum in PBS) at room temperature in a humidified chamber. Subsequently, sections were
306 incubated overnight at 4°C with primary polyclonal antibodies. The antibody to Chromogranin
307 A (1:100), T1R2 (1:200) and T1R3 (1:200). The T1R2 antibody was raised against a peptide
308 corresponding to residues 426-570 of mouse T1R2 that shares 66% homology with rabbit
309 T1R2, and T1R3 to a peptide corresponding to the c-terminus of human T1R3. Cloned rabbit
310 T1R3 shares 69% homology to human T1R3. After incubation of sections with primary
311 antibodies, slides were washed five times for 5 minutes each in PBS and subsequently stained
312 for 1 hour at room temperature using a 1:500 dilution of Cyanine 3 (Cy3)- or Fluorescein
313 isothiocyanate (FITC)-conjugated anti-goat, anti-rabbit and anti-mouse IgG secondary
314 antibodies. The composition of the buffer containing antibodies (primary or secondary) was
315 2.5% (v/v) donkey serum, 0.25% (w/v) NaN_3 , and 0.2% (v/v) Triton X-100 in PBS. Finally,
316 slides were washed five times for 5 minutes each in PBS and then mounted with Vectashield
317 Hard Set Mounting Medium with (DAPI). Immunofluorescent labeling of Chromogranin A,

318 T1R2 and T1R3 proteins was visualized using an epifluorescence microscope (Nikon,
319 Kingston-Upon-Thames, UK), and images were captured with a digital camera (model C4742-
320 96-12G04, Hamamatsu Photonics, Welwyn Garden City, UK). Omission of primary antibodies
321 was routinely used as the control.

322

323 **Statistical Analysis.** All parameters were tested for normality by the Shapiro–Wilk test. For
324 comparison of SGLT1 expression in intestinal tissues and measurements of crypt-depth/villus
325 height in intestinal tissues a Student’s two-tailed t-test was used to determine statistical
326 significance (GraphPad Prism 5, GraphPad Software Inc., La Jolla, CA). The level of
327 statistical significance was set at $p < 0.05$.

328

329

330 RESULTS

331 Phase 1 studies

332 **Assessment of rabbit performance.** Rabbit daily weight gain, feed intake, and gain to feed
333 ratios are presented in Figure 1. *E-coli* inoculation markedly decreased daily weight gain ($p <$
334 0.001 ; Figure 1A) across all dietary treatments until surviving animals had recovered by day
335 19 post infection (63 days of age). There was no effect of dietary supplementation on daily
336 weight gain ($p > 0.70$; Figure 1A). Feed intake was not affected by inoculation Figure 1B).
337 There was a trend for an effect of dietary treatment ($p < 0.10$) such that the animals
338 supplemented with 75 ppm SL consumed more feed in the middle of the clinical phase of
339 disease (day 12 post infection; 56 days of age; Figure 1B). Inoculation markedly decreased
340 efficiency of growth ($p < 0.001$; Figure 1C) and this was not influenced by dietary treatment
341 ($p > 0.50$). None of the groups recovered to pre-inoculation feed efficiency for the duration of
342 the study.

343

344 **Mortality and morbidities.** Rabbit rates of mortality are presented in Figure 2. The
345 colibacillosis challenge had a strong effect and elicited a marked increase in mortality rate (p
346 < 0.001 ; Figure 2A), with peak levels reached on day 19 post infection (63 d of age). There
347 was no effect of dietary treatment on percent rate of mortality ($p > 0.30$); however, the 75
348 ppm SL group had nearly half the mortality rate of the control group. Cumulative death was
349 increased by inoculation ($p < 0.001$; Figure 2B), and the number of dead animals tended to
350 decrease with doses of 50 and 75 ppm ($p < 0.20$; Figure 2B). The average body weight on
351 day 26 post infection (70 d of age) was multiplied by the number of animals alive on that day
352 to give production weights of 112.5, 119.2, 121.2, and 111.9 g for animals supplemented with
353 0, 50, 75, and 100 ppm SL, respectively.

354 Morbidities (diarrhea and bloat) are presented in Figure 3. The majority of morbidities
355 observed were diarrhea, and this was increased with inoculation ($p < 0.001$; Figure 3A). All
356 animals reached pre-inoculation levels by day 26 post infection (70 d of age) and there was
357 no effect of dietary treatment on percent morbidities ($p > 0.40$; Figure 3A). The cumulative
358 number of morbidities also increased with inoculation ($p < 0.001$; Figure 3B) and there was a
359 significant treatment effect characterized by fewer morbid animals in the 50 and 75 ppm SL
360 groups, compared to control animals ($p < 0.01$; Figure 3B).

361

362 **Phase 2 studies**

363 **Rabbit SGLT1 expression and activity is enhanced by feed supplementation with the**

364 **natural high-intensity sweetener, stevia leaf.** SGLT1 expression and activity was

365 determined along the length of the small intestine in rabbits, fed a diet supplemented with SL

366 and the same diet without SL (control diet). Irrespective of diets, levels of SGLT1 mRNA,

367 protein and function were highest in the duodenum>jejunum>ileum. There was a 1.4- ($p <$

368 0.05) and 1.3-fold ($p < 0.001$) increase in SGLT1 mRNA abundance in the duodenum and

369 jejunum of rabbits fed a diet supplemented with SL compared to control diet (Figure 4A).

370 SGLT1 protein abundance measured in BBMV increased by 1.6- ($p < 0.001$) and 1.6-fold (p

371 < 0.001) in the duodenum and jejunum of rabbits fed a diet supplemented with SL compared

372 to control (Figure 4B). This was matched by 1.8- ($p < 0.050$) and 1.7-fold ($p < 0.050$)

373 increase in the initial rates of D-glucose transport into BBMV in the duodenum and jejunum

374 of rabbits fed a diet supplemented with SL compared to the control diet (Figure 4C). No

375 increases in either SGLT1 mRNA, protein abundance, or the initial rate of D-glucose

376 transport into BBMV were observed in the ileum of rabbits fed a diet supplemented with SL,

377 compared to control diet (Figure 4). There was a 1.4- ($p < 0.0010$) and 1.3-fold ($p < 0.0010$)

378 increase in villus height in the duodenum and jejunum of SL fed rabbits compared to controls

379 (Figure 5). There was no difference in the average villus heights of control and SL fed rabbits
380 in the ileum.

381

382 **Expression of T1R2 and T1R3 in the rabbit intestine.** For rabbit T1R2, PCR primers were
383 designed against the predicted mRNA sequence available on the National Center for
384 Biotechnology Information (NCBI) non-redundant nucleotide database. PCR amplicons using
385 rabbit jejunal cDNA and the designed T1R2 primers resulted in a 152 bp amplicon, which
386 was found to be a 100% match to the predicted NCBI sequence, revealing that rabbit intestine
387 expresses T1R2 (Figure 6). An alignment of the full-length rabbit T1R2 mRNA sequence
388 showed 55.3% homology with cow, pig, human, mouse and rat T1R2.

389

390 As no sequence information on rabbit T1R3 was available from the current release of the
391 rabbit genome (NCBI OryCun2.0 Annotation Release 102), it was necessary to clone rabbit
392 T1R3 to obtain mRNA sequence data and verify its expression in the rabbit intestine. PCR
393 amplification using rabbit jejunal cDNA and consensus mammalian T1R3 primers resulted in
394 a 1221 bp fragment that was screened against the National Center for Biotechnology
395 Information (NCBI) non-redundant nucleotide database, via BlastN,²³ identifying the
396 amplified sequence as being homologous to T1R3 in many other mammalian species. The
397 mRNA fragment was subsequently translated to produce a sequence of 407 amino acids
398 (corresponding to residues 116-515 of human T1R3). Phylogenetic analysis was performed to
399 construct a radial phylogram depicting the relationship of rabbit T1R3 to homologs in various
400 other mammalian species for which sequence information was available (Figure 7). The
401 NCBI accession number for the mRNA sequence of rabbit T1R3 is MK182098.

402

403 Immunofluorescence detection for the sweet receptor subunits, T1R2 and T1R3, as well as
404 the classical marker for enteroendocrine cells, chromogranin A, was performed on frozen
405 tissue sections of rabbit duodenum and jejunum. As shown in figure 8, T1R2 and T1R3 were
406 co-expressed in the same cell (Figure 8A). Furthermore, both T1R2 and T1R3 were co-
407 expressed with chromogranin A, confirming receptor subunits expression in the
408 enteroendocrine cell (Figure 8B).

409

410 **DISCUSSION**

411 Feeding of low-level antibiotics has been a routine procedure for controlling enteric
412 pathogens, preventing disease, improving health and growth, in particular in post weaning-
413 animals.²⁴ However, increasing antibiotic resistance and rising consumer concern over
414 prophylactic antibiotic use in animal production has led to a concerted search for effective
415 alternatives. In humans, oral rehydration therapy, which relies on absorption of glucose via
416 SGLT1, activating electrolyte and water absorption is a safe and effective method for the
417 treatment of *E-coli*- and *Vibrio cholerae*- induced diarrhea.¹ The discovery that sensing of
418 sugars and sweeteners by the gut-expressed sweet receptor T1R2-T1R3 enhances the
419 expression and activity of SGLT1,⁴ has allowed the design of novel strategies for animal
420 nutrition that use artificial sweeteners to combat diarrheal and enteric diseases.²⁵

421 *E. coli*- induced diarrhea is endemic in rabbits and results in high rates of morbidity and
422 mortality. In the EU, artificial sweeteners are not permitted to be used in rabbit feed.

423 We hypothesized that rabbit intestine expresses the intestinal sweet receptor T1R2-T1R3, and
424 that a natural high intensity sweetener (stevia) activates the receptor leading to SGLT1
425 upregulation improving *E-coli*-induced enteric disorders. The supplement used in this study
426 contained a small amount (2%) of *capsicum oleoresin* (~ 4.9 μ M capsaicin) shown to
427 influence immunity. However, using heterologous expression of rabbit T1R2-T1R3 we have

428 determined that capsaicin does not activate rabbit T1R2-T1R3. In contrast, stevia leaf extract
429 (SL) activates the receptor in a dose-dependent manner (unpublished data, paper in
430 preparation).

431 Work in the laboratory of Tavakkolizadeh and colleagues^{26,27} have questioned the role of
432 vagal afferent fibres in SGLT1 regulation by vagotomy and de-afferentation with 1 mg
433 capsaicin applied per animal. They have concluded that vagal de-afferentation abolishes SGLT1
434 upregulation in response to increased luminal glucose. They have further proposed that the
435 specific involvement of vagal afferent fibres and enteric nervous system in glucose-sensing
436 initiated regulatory pathway controlling SGLT1 expression remains unclear.²⁷

437 Bates, Sharkey and Meddings 1998,²⁸ have shown that guinea pigs treated with vehicle, and
438 thus having intact vagal afferent were able to increase the ability to enhance intestinal glucose
439 transport when switched from a low- to a high-carbohydrate containing diet. In contrast,
440 animals that received 32.8 mM solution of capsaicin demonstrated no adaptation to
441 alterations in dietary composition.²⁸ Interestingly Nassar et al. 1995,²⁹ have shown that
442 capsaicin (160 and 800 μ M) reduces significantly intestinal alanine absorption when perfused
443 either intraluminally or applied topically to the vagus nerve, concluding the involvement of
444 vagal capsaicin sensitive primary afferent fibres in this inhibitory mechanism.²⁹ Thus, it
445 appears that vagal de-afferentiation may have a generalized effect on inhibiting a range of
446 intestinal nutrient absorptive processes.

447 The results of studies carried out by Streamer et al., 2010 and Bates et al., 1998 are in contrast
448 to this study. In our study, rabbits fed diets that included stevia and capsaicin (maximum
449 capsaicin concentration, 4.9 μ M) were able to upregulate glucose transporter
450 expression/activity compared to those fed the same diet without capsaicin.

451 We have shown recently that electric field stimulation of an isolated segment of the intestine
452 results in 2-3 fold increase in SGLT1 upregulation.⁶ This increase is abolished in presence of

453 the nerve blocking agent tetrodotoxin, indicating the involvement of enteric nervous system
454 in the regulatory pathway. We used this strategy because sensing of glucose or artificial
455 sweeteners via T1R2-T1R3, expressed in enteroendocrine cells, stimulates GLP-2 release, and
456 GLP-2 via binding to its receptor (GLP-2R) present in enteric neurons induces an action
457 potential.³⁰ We showed that electric field stimulation of enteric neurons, induces a neural
458 response leading to secretion of specific neuropeptides that upregulate SGLT1 expression in
459 the neighbouring absorptive enterocyte, by enhancing half-life of SGLT1 mRNA and thus
460 increased in SGLT1 protein abundance⁶. Our studies strongly supports the involvement of
461 enteric neurons in a glucose-sensing initiated pathway regulating SGLT1 expression.⁶
462 Additional studies are required to address if there is a specific involvement of vagus nerve
463 in SGLT1 regulatory pathway.

464 In this study we determined the effect of supplementation of feed with an additive containing
465 SL on rabbit intestinal SGLT1 expression, as sweeteners are known to enhance Na⁺-
466 dependent glucose absorption in other mammalian species.^{4,12,13} Since the regulatory pathway
467 controlling SGLT1 expression/function is initiated by activation of the gut-expressed sweet
468 receptor T1R2-T1R3, we aimed to identify if these receptor subunits were expressed in the
469 rabbit intestine. The gene for rabbit T1R2 has previously been identified from the rabbit
470 genome sequence, located on chromosome 13 (NCBI OryCun2.0 Annotation Release 102);
471 however, no information was available for rabbit T1R3. To determine expression of T1R2
472 and T1R3 in rabbit intestine, a PCR based strategy was used to demonstrate that rabbit
473 intestine does indeed express both receptor subunits T1R2 and T1R3 at mRNA level.

474 Moreover, by immunohistochemistry we showed that T1R2, T1R3 proteins are co-expressed
475 in the same intestinal enteroendocrine cell. Furthermore, SGLT1 mRNA, protein abundance
476 and glucose transport function were increased ~2-fold by dietary inclusion of SL, providing a
477 higher capacity for the rabbit intestine to absorb glucose, electrolyte and water. There was

478 also 1.4-fold increase in villus height in rabbits consuming SL, likely due to GLP-2 action.¹³
479 In these dietary studies, we maintained rabbits on diets with and without SL for 9 days. We
480 have shown SGLT1 upregulation, with a similar increase in magnitude after 1 day or 5 day in
481 response to increased dietary carbohydrates or sweeteners^{4,6}, indicating that increase in
482 SGLT1 expression occurs in existing absorptive enterocytes.^{6,7} However, since this was the
483 first time that we were assessing potential SGLT1 upregulation in response to inclusion of a
484 natural sweetener in the feed of rabbits, we selected a 5-day dietary trial in order to cover
485 intestinal epithelial cell turnover that takes 4-5 days in the majority of species. This period
486 was extended to 9 days because of the researcher travel delays from the UK to France for
487 harvesting rabbit intestinal tissues.

488 We also assessed the effect of supplementation of rabbit feed with SL on relieving *E. coli*-
489 induced enteric disorders and observed that inclusion of SL in the feed decreases morbidity
490 associated with disease. Although we did not observe a linear dose response, there was a
491 clear trend for improved morbidities at the two lower doses. Such hormetic responses to
492 plant-based supplements are common; very low doses are beneficial whereas higher doses are
493 non-specific and detrimental³¹. To our knowledge this is the first report evaluating the effect
494 of a natural artificial sweetener on rabbit health and performance, and the associated
495 molecular mechanisms.

496 The *E. coli* challenge elicited a marked impact on performance, characterized by blunted feed
497 intake, decreased daily gain, and efficiency of growth. These are classical signs of infection
498 that not only lead to stressed animals but have a devastating economic impact in rabbit
499 production. The use of artificial sweetener to prevent decreased performance during stress
500 has been explored previously. For example, Sterk et al.³² reported that supplementation of
501 weanling piglets with artificial sweetener prevented the decrease in feed intake around
502 weaning. Similar observations have been made for receiving feedlot cattle with respect to

503 both feed intake³³ and daily weight gain.³⁴ Whilst in this study the inclusion of SL in the feed
504 had some impact on feed intake, the major effect is at the gut level where activation of gut-
505 expressed T1R2-T1R3 by sweeteners results in the secretion of GLP-2, a gut hormone that
506 can alter appetite,³⁵ and also the intestinal uptake of glucose leading to improved efficiency
507 of growth.⁶ It has indeed been shown that artificial sweeteners directly introduced into the
508 lumen of the intestine, bypassing the oral cavity, lead to an increase in expression of SGLT1
509 and higher rates of intestinal glucose absorption.²⁷

510 It was noteworthy that the *E. coli* challenge in this study was quite severe, with mortality rate
511 peaking at nearly 60% during the clinical trials in some groups. Despite the severity of the
512 disease challenge, the supplement showed a trend for a positive effect on cumulative
513 morbidities at the lower doses. This observation was consistent with those we made during
514 our preliminary experiments to establish the optimal timing and dose of inoculation (data not
515 shown). Previous work using an artificial high-intensity sweetener has revealed similar
516 effects during enteric disease challenge,³⁶ but this is the first report on the impact of a natural
517 high-intensity sweetener for prevention of clinical signs of enteritis in rabbits. The positive
518 impact of the supplement on morbidities, combined with the molecular responses we
519 observed, are consistent with an increase in GLP-2 secretion which is known to be essential
520 for gut repair after injury,²⁵ and also an enhancement in nutrient absorption.⁶ In this scenario,
521 the increased glucose, electrolyte and water absorption at the intestinal level likely decreased
522 the clinical signs of disease associated with diarrhea, and the enteric lesions caused by the
523 pathogen were likely reduced or repaired in supplemented animals due to GLP-2 effect.

524

525 **AUTHOR INFORMATION**

526 **Corresponding Author**

527 *S.P.S-B.: tel, +44 151 794 4255; e-mail, spsb@liverpool.ac.uk

528 **Author contributions**

529 ⊥A.W.M. and M.A.A-R. contributed equally to this work.
530 S.P.S-B. is responsible for conception of studies described in phase-2, with A.W.M.
531 designing and carrying out experiments on isolating rabbit intestinal BBMV, western
532 blotting, glucose transport function, morphometric analyses and determining intestinal
533 expression of T1R2. M.A.A-R. performed immunohistochemistry. K.D. cloned and
534 sequenced rabbit T1R3. S.P.S-B., A.W.M. and K.D. analyzed and interpreted the data. E.G.
535 carried out feed trial studies described in phase 1 and -2 of the study. C.I. assisted with the
536 experimental design, and D.M.B. conceptualized the project and the potential application of
537 the supplement in rabbits. E.H.W. designed, directed, discussed phase-1 and -2 animal studies
538 and commented on the paper. S.P.S-B. wrote the paper.
539

540 **REFERENCES**

- 541 (1) Hirschhorn, N.; Greenough, W. B. Progress in oral rehydration therapy. *Scientific*
542 *American*. **1991**, 264, 50-56.
- 543 (2) Hamilton, H.L. Robert K. Crane-Na(+)-glucose cotransporter to cure? *Front Physiol*.
544 **2013**, 4, 53.
- 545 (3) Dyer J.; Salmon, K. S.; Zibrik, L.; Shirazi-Beechey, S. P. Expression of sweet taste
546 receptors of the T1R family in the intestinal tract and enteroendocrine cells. *Biochem. Soc.*
547 *Trans*. **2005**, 33, 302-305.
- 548 (4) Margolskee R. F.; Dyer, J.; Kokrashvili, Z.; Salmon, K. S.; Ilegems, E.; Daly, K.; Maillet,
549 E. L.; Ninomiya, Y.; Mosinger, B.; Shirazi-Beechey, S. P. T1R3 and gustducin in gut sense
550 sugars to regulate expression of Na⁺-glucose cotransporter 1. *Proc. Natl. Acad. Sci. USA*.
551 **2007**, 104, 15075-15080.
- 552 (5) Jang, H.J.; Kokrashvili, Z.; Theodorakis, M.J.; Carlson, O.D.; Kim, B.J.; Zhou, J.; Kim,
553 H.H.; Xu, X.; Chan, S.L.; Juhaszova, M.; Bernier, M.; Mosinger, B.; Margolskee, R.F.; Egan,
554 J.M. Gut-expressed gustducin and taste receptors regulate secretion of glucagon-like peptide-
555 1. *Proc Natl Acad Sci U. S. A*. **2007**, 104, 15069-74.
- 556 (6) Moran, A. W.; Al-Rammahi, M. A.; Batchelor, D. J.; Bravo, D. M.; Shirazi-Beechey, S.
557 P. Glucagon-Like Peptide-2 and the Enteric Nervous System Are Components of Cell-Cell
558 Communication Pathway Regulating Intestinal Na⁺/Glucose Co-transport. *Front. Nutr*. **2018**,
559 5, 101.
- 560 (7) Cheeseman, C.I. Upregulation of SGLT-1 transport activity in rat jejunum induced by
561 GLP-2 infusion in vivo. *Am J Physiol Regul Integr Comp Physiol*. **1997**, 273(6), R1965-71.
- 562 (8) Burrin, D.; Guan, X.; Stoll, B.; Petersen, Y.M.; Sangild, P.T. Glucagon-like peptide 2: a
563 key link between nutritional and intestinal adaptation in neonates? *J Nutr*. **2003**, 133, 3712-6.
- 564 (9) Shirazi-Beechey, S. P.; Moran, A. W.; Batchelor, D. J.; Daly, K.; Al-Rammahi, M.
565 Glucose sensing and signalling; regulation of intestinal glucose transport. *Proc. Nutr. Soc*.
566 **2011**, 70, 185-193.
- 567 (10) Brubaker, P.L. Glucagon-like Peptide-2 and the Regulation of Intestinal Growth and
568 Function. *Compr Physiol*. **2018**, 8, 1185-1210.
- 569 (11) Ren, W.; Wu, J.; Li, L.; Lu, Y.; Shao, Y.; Qi, Y.; Xu, B.; He, Y.; Hu, Y. Glucagon-Like
570 Peptide-2 Improve Intestinal Mucosal Barrier Function in Ages Rats. *J Nutr Health Aging*.
571 **2018**, 22, 731-738.
- 572 (12) Moran, A. W.; Al-Rammahi, M. A.; Arora, D. K.; Batchelor, D. J.; Coulter, E. A.; Daly,
573 K.; Ionescu, C.; Bravo, D.; Shirazi-Beechey, S. P. Expression of sodium/glucose co-
574 transporter 1 (SGLT1) is enhanced by supplementation of the diet weaning piglets with
575 artificial sweeteners. *Br. J. Nutr*. **2010**, 104, 637-646.
- 576 (13) Moran, A.W.; Al-Rammahi, M.; Zhang, C.; Bravo, D.; Calsamiglia, S.; Shirazi-Beechey,
577 S. P. Sweet taste receptor expression in ruminant intestine and its activation by artificial
578 sweeteners to regulate glucose absorption. *J. Dairy Sci*. **2014**, 97, 4955-4972.

- 579 (14) Bojahr, J.; Brockhoff, A.; Daly, K.; Meyerhof, W.; Shirazi-Beechey, S. Characterization
580 of the pig sweet taste receptor by heterologous expression. *Chem senses*. **2015**, 40(3), 270-
581 271.
- 582 (15) Saitou, N.; Nei, M. The neighbor-joining method: a new method for reconstructing
583 phylogenetic trees. *Mol. Biol. Evol.* **1987**, 4, 406-425.
- 584 (16) Jones D. T.; Taylor, W. R.; Thornton, J. M. The rapid generation of mutation data matrices
585 from protein sequences. *Comput. Appl. Biosci.* **1992**, 8, 275-282.
- 586 (17) Felsenstein, J. PHYLIP - Phylogeny Inference Package (Version 3.2). *Cladistics*. **1989**,
587 5, 164-166.
- 588 (18) Ye, J.; Coulouris, G.; Zaretskaya, I.; Cutcutache, I.; Rozen, S.; Madde, T. Primer-
589 BLAST: A tool to design target-specific primers for polymerase chain reaction. *BMC*
590 *Bioinformatics* **2012**, 13, 134.
- 591 (19) Shirazi-Beechey, S. P.; Davies, A. G.; Tebbutt, K.; Dyer, J.; Ellis, A.; Taylor, C. J.;
592 Fairclough, P.; Beechey, R. B. Preparation and properties of brush-border membrane vesicles
593 from human small intestine. *Gastroenterology*. **1990**, 98, 676-685.
- 594 (20) Rowell-Schäfer, A.; Dyer, J.; Hofmann, R. R.; Lechner-Doll, M.; Meyer, H. H. D.;
595 Shirazi-Beechey, S. P.; Streich, W. J. Abundance of intestinal Na⁺/glucose cotransporter
596 (SGLT1) in roe deer (*Capreolus capreolus*). *J. Animal Physiol. a. Animal Nutrition*. **1999**, 82,
597 25-32.
- 598 (21) Dyer, J.; Vayro, S.; King, T. P.; Shirazi-Beechey, S. P. Glucose sensing in the intestinal
599 epithelium. *Eur. J. Biochem.* **2003**, 270, 3377-3388.
- 600 (22) Dyer, J.; Al-Rammahi, M.; Waterfall, L.; Salmon, K. S.; Geor, R. J.; Bouré, L.;
601 Edwards, G. B.; Proudman, C. J.; Shirazi-Beechey, S. P. Adaptive response of equine
602 intestinal Na⁺/glucose co-transporter (SGLT1) to an increase in dietary soluble carbohydrate.
603 *Pflugers Arch. – Eur. J. Physiol.* **2009**, 458, 419-430.
- 604 (23) Johnson, M.; Zaretskaya, I.; Raytselis, Y.; Merezhuk, Y.; McGinnis, S.; Madden, T. L.
605 NCBI BLAST: a better web interface. *Nucleic Acids Res.* **2008**, 36(Web Server issue), W5-9.
- 606 (24) Rhouma, M.; Fairbrother, J. M.; Beaudry, F.; Letellier, A. Post weaning diarrhea in pigs:
607 risk factors and non-colistin-based control strategies. *Acta Vet Scand.* **2017**, 59(1), 31.
- 608 (25) Connor E. E.; Evoke-Clover, C. M.; Wall, E. H.; Baldwin 6th, R. L.; Santin-Duran, M.;
609 Elsasser, T. H.; Bravo, D. M. Glucagon-like peptide 2 and its beneficial effects on gut
610 function and health in production animals. *Domest Anim Endocrinol.* **2016**, 56 Suppl, S56-65.
- 611 (26) Stearns, A.T.; Balakrishnan, A.; Rounds, J.; Rhoads, D.B.; Ashley, S.W.;
612 Tavakkolizadeh, A. Capsaicin-sensitive vagal afferents modulate posttranscriptional
613 regulation of the rat Na⁺/glucose cotransporter SGLT1. *Am J Physiol Gastrointest Liver*
614 *Physiol.* **2008**, 294(4), G1078-83.
- 615 (27) Stearns, A.T.; Balakrishnan, A.; Rhoads, D.B.; Tavakkolizadeh, A. Rapid upregulation
616 of sodium-glucose transporter SGLT1 in response to intestinal sweet taste stimulation. *Ann*
617 *Surg.* **2010**, 251(5), 865-71.

- 618 (28) Bates, S.L.; Sharkey, K.A.; Meddings, J.B. Vagal involvement in dietary regulation of
619 nutrient transport. *Am J Physiol.* **1998**, 274(3), G552-60.
- 620 (29) Nassar, C.F.; Barada, K.A.; Abdallah, L.E.; Hamdan, W.S.; Taha, A.M.; Atweh, S.F.;
621 Saadé, N.E. Involvement of capsaicin-sensitive primary afferent fibers in regulation of jejunal
622 alanine absorption. *Am J Physiol.* **1995**, 268(4), G695-9.
- 623 (30) Mills, J.C.; Gordon, J.I. The intestinal stem cell niche: there grows the neighborhood.
624 *Proc Natl Acad Sci USA*, **2001**, 98,12334-6.
- 625 (31) Lillehoj, H.; Liu, Y.; Calsamiglia, S.; Fernandez-Miyakawa, M.E.; Chi, F.; Cravens,
626 R.L.; Oh, S.; Gay, C.G. Phytochemicals as antibiotic alternatives to promote growth and
627 enhance host health. *Vet Res.* **2018**, 49, 76.
- 628 (32) Sterk A.; Schlegel, P.; Mul, A. J.; Ubbink-Blanksma, M.; Bruininx, E. M. Effects of
629 sweeteners on individual feed intake characteristics and performance in group-housed
630 weanling pigs. *J Anim Sci.* **2008**, 86(11), 2990-7.
- 631 (33) Ponce C.H.; Brown, M. S.; Silva, J. S.; Schlegel, P.; Rounds, W.; Hallford, D. M.
632 Effects of a dietary sweetener on growth performance and health of stressed beef calves and
633 on diet digestibility and plasma and urinary metabolite concentrations of healthy calves. *J*
634 *Anim Sci.* **2014**, 92(4), 1630-8.
- 635 (34) McMeniman J.P.; Rivera, J. D.; Schlegel, P.; Rounds, W.; Galyean, M. L. Effects of an
636 artificial sweetener on health, performance, and dietary preference of feedlot cattle. *J Anim*
637 *Sci.* **2006**, 84(9), 2491-500.
- 638 (35) Baldassano, S.; Amato, A.; Mulè, F. Influence of glucagon-like peptide 2 on energy
639 homeostasis. *Peptides.* **2016**, 86, 1-5.
- 640 (36) Connor, E. E.; Wall, E. H.; Bravo, D. M.; Evock-Clover, C. M.; Elsasser, T. H.; Baldwin
641 6th, R. L.; Santín, M.; Vinyard, B. T.; Kahl, S.; Walker, M. P. Reducing gut effects from
642 *Cryptosporidium parvum* infection in dairy calves through prophylactic glucagon-like peptide
643 2 therapy or feeding of an artificial sweetener. *J. Dairy Sci.* **2017**, 100(4), 3004-3018.
- 644
645

646 **Figure 1.** Growth performance of rabbits supplemented with 0, 50, 75, or 100 ppm of an
647 additive containing natural high-intensity sweetener (SL) and inoculated with *Escherichia*
648 *coli* on day 44 of age (red arrow). Data presented are LS Means, with SEM indicated on each
649 panel. A, daily weight gain; B, daily feed intake; C, gain:feed.

650 **Figure 2.** Mortality of rabbits supplemented with 0, 50, 75, or 100 ppm of an additive
651 containing natural high-intensity sweetener (SL) and inoculated with *Escherichia coli* on day
652 44 of age (red arrow). A, percent mortality over time. B, total number of dead animals over
653 time. Mortality was calculated by dividing the number of new deaths recorded at each time
654 point by the number of animals alive at the previous time point, and then multiplying by 100.

655 **Figure 3.** Morbidity (diarrhea, abnormal feces, and/or bloat) of rabbits supplemented with 0,
656 50, 75, or 100 ppm of an additive containing natural high-intensity sweetener (SL) and
657 inoculated with *Escherichia coli* on day 44 of age (red arrow). A, percent morbidity over
658 time. B, cumulative morbidity over time. * = $p < 0.05$; ** = $p < 0.01$

659 **Figure 4. Expression and activity of SGLT1 in the intestine of control rabbits and in**
660 **rabbits maintained on the same diet supplemented with SL.** Brush border membrane
661 vesicles (BBMV) and RNA were isolated from small intestinal tissues of rabbits fed either a
662 control diet (C) or a diet supplemented with an additive containing natural high-intensity
663 sweetener (SL). A: Level of SGLT1 mRNA abundance normalized to β -actin, RNA
664 polymerase II and β -2-microglobulin mRNA. B: Expression of SGLT1 and β -actin proteins
665 in BBMV isolated from the small intestine assessed by western blotting (*left panel*).
666 Densitometric analysis of SGLT1 protein abundance normalized to β -actin (*right panel*). C:
667 Initial rates of Na^+ -dependent [^{14}C]-D-glucose uptake into BBMV. Data were generated in
668 triplicate. Results are shown as mean \pm SEM; $n = 7$ animals. Statistically significant results

669 determined using a Student's two-tailed t-test where * = $p < 0.050$; ** = $p < 0.010$; *** = p
670 < 0.001 .

671 **Figure 5. Morphometric analysis of the rabbit intestine.** A) Representative light
672 micrographs of small intestinal tissues of control and natural high-intensity sweetener (SL)
673 fed rabbits. Images were obtained at 4X magnification. B) Morphometric analyses of villus
674 height and crypt depths are shown as histograms, in (μm) \pm SEM. Control (\square), SL-fed (\blacksquare); n
675 = 5 animals. Statistically significant results were determined using Student's two-tailed t-test
676 where ** = $p < 0.010$.

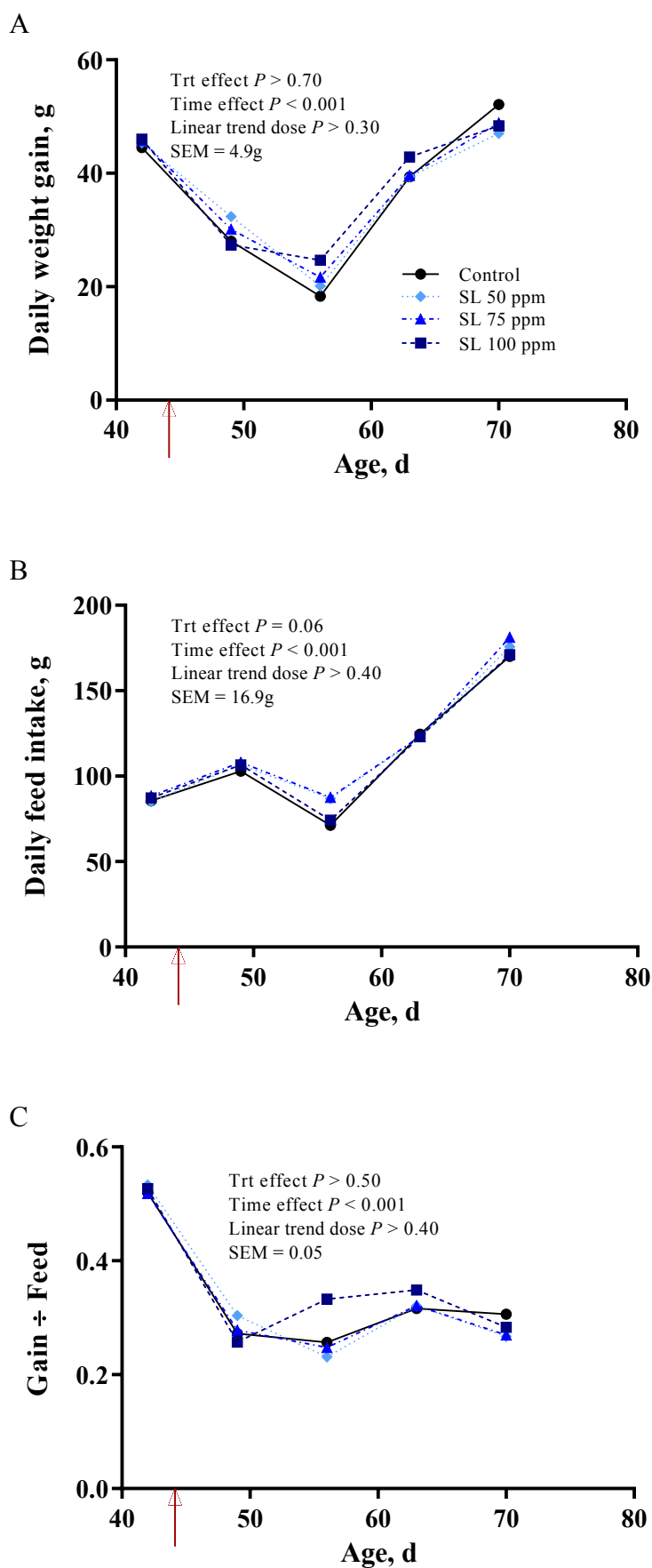
677 **Figure 6.** Alignment of rabbit T1R2 mRNA sequence with the corresponding region of cow,
678 pig, human, mouse and rat T1R2 (numbers in parentheses relate to initiating nucleotide).

679 **Figure 7.** Radial phylogram, derived from amino acid sequences, depicting the phylogenetic
680 relationship of rabbit T1R3 to various mammalian homologs. The scale bar represents the
681 number of substitutions per amino acid position.

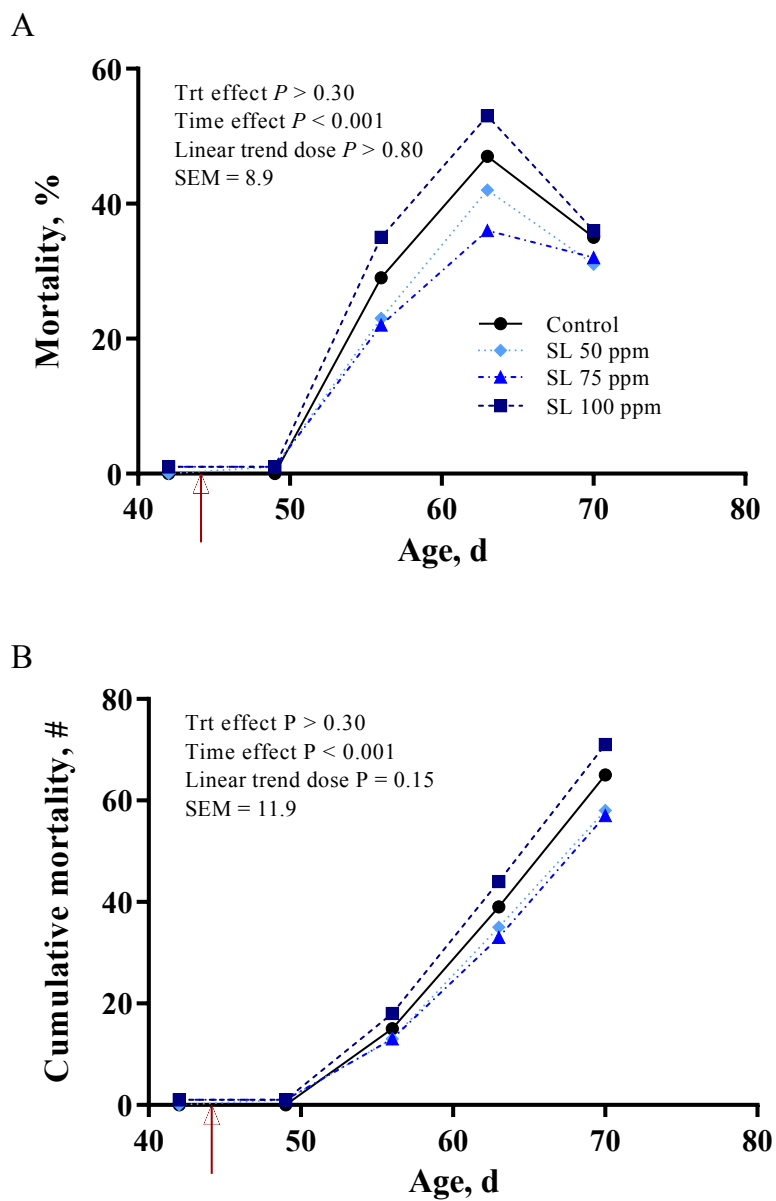
682 **Figure 8. Co-expression of T1R2 and T1R3 in rabbit small intestine.** A) A representative
683 image shows expression of T1R2 (green), T1R3 (red) and merged image (yellow) in serial
684 sections of rabbit small intestine as determined by double immunohistochemistry. B) A
685 typical image showing expression of T1R2 or T1R3 (green), the enteroendocrine marker,
686 chromogranin A (ChA, red) and merged image (yellow). Specificity of primary antibodies for
687 T1R2 and T1R3 have been validated in mice.⁶ Omission of primary antibodies for T1R2 or
688 T1R3 showed no non-specific immunoreactivity with secondary antibodies. (-T1R2 control
689 & -T1R3 control). All images were taken under 400X magnification, scale bar represents 20
690 μm .

691

692

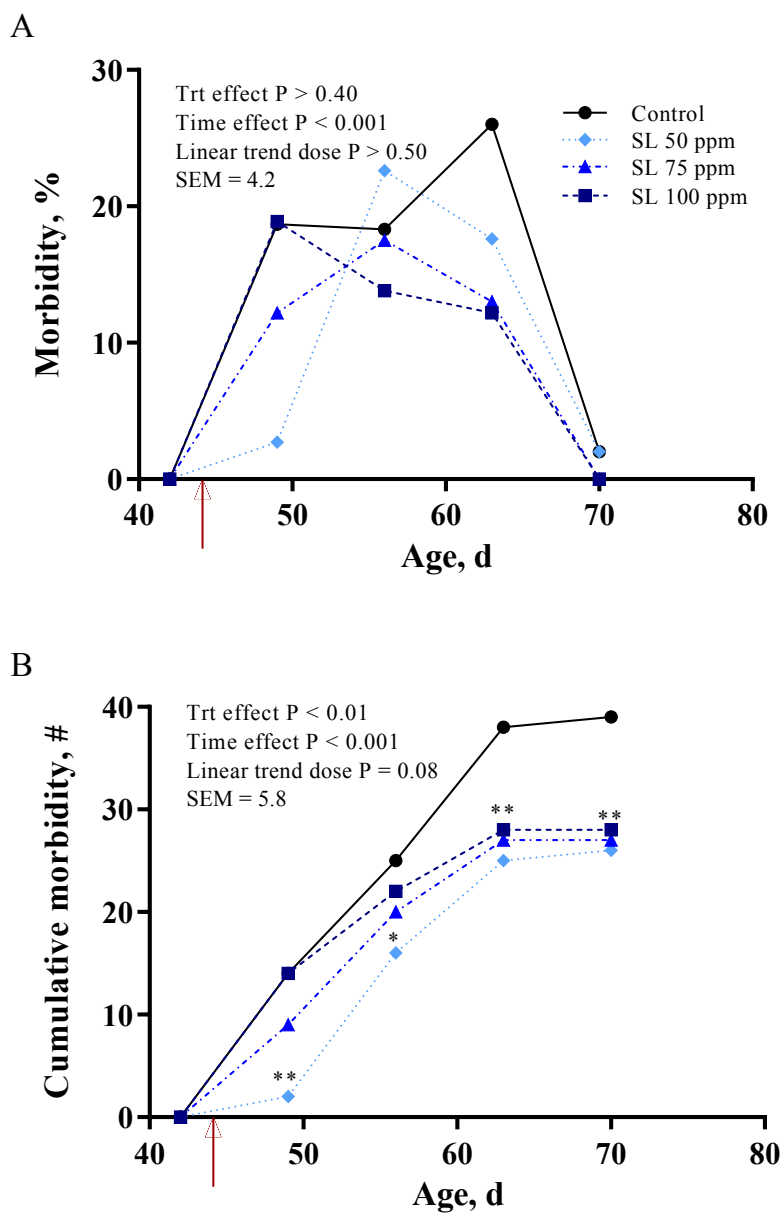


693 Figure 1

694 **Figure 2**

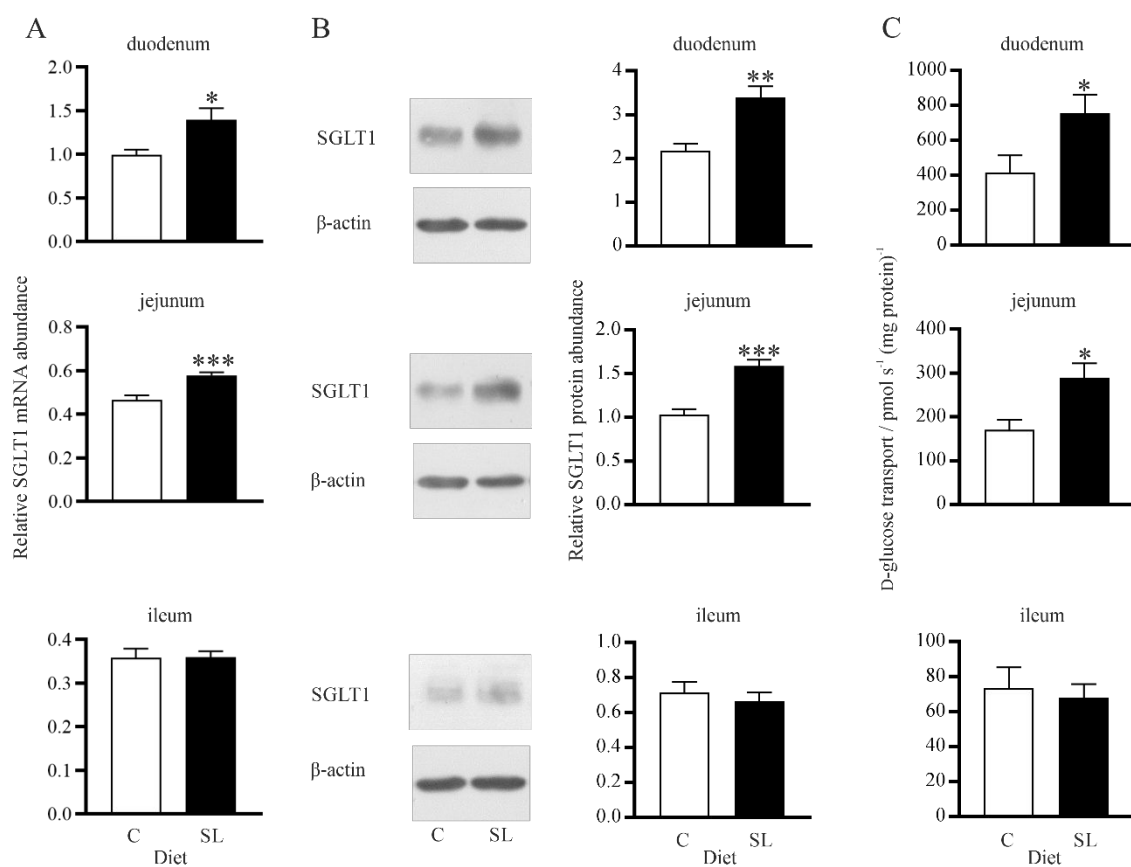
695

696

697 **Figure 3**

698

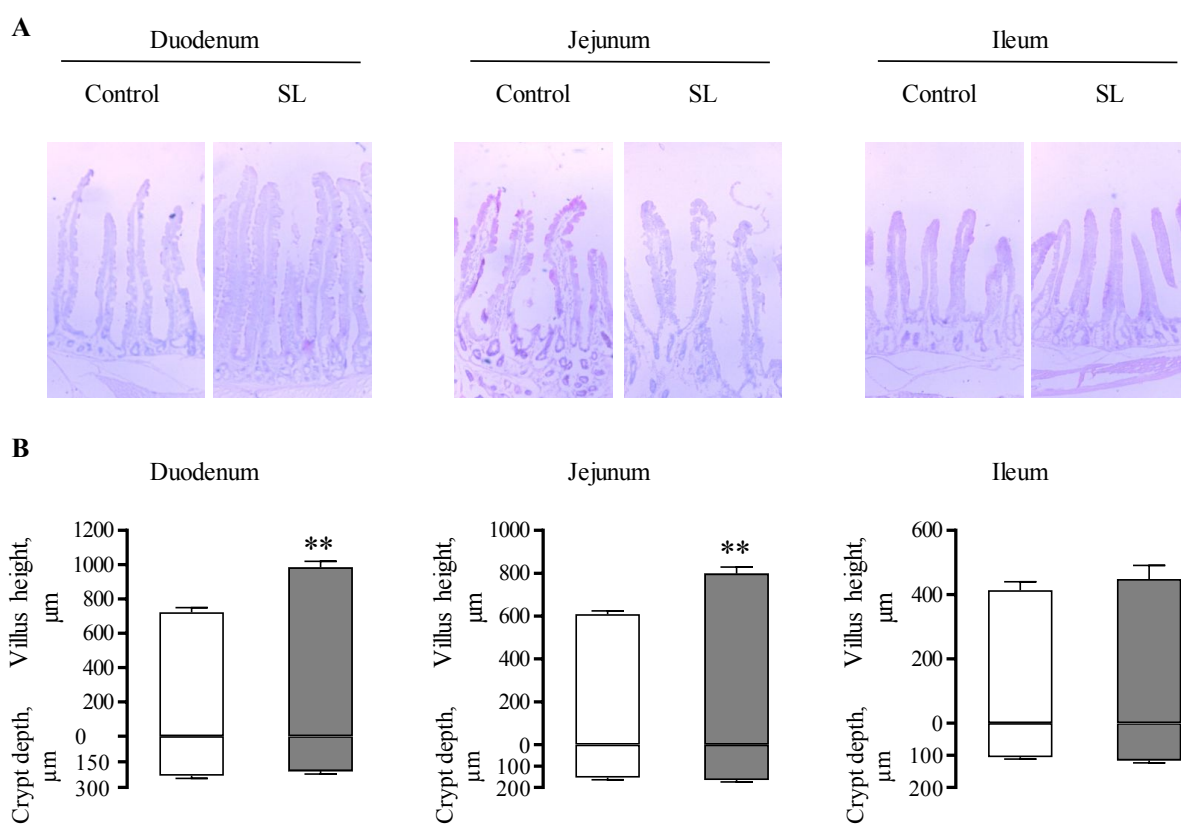
699

700 **Figure 4**

701

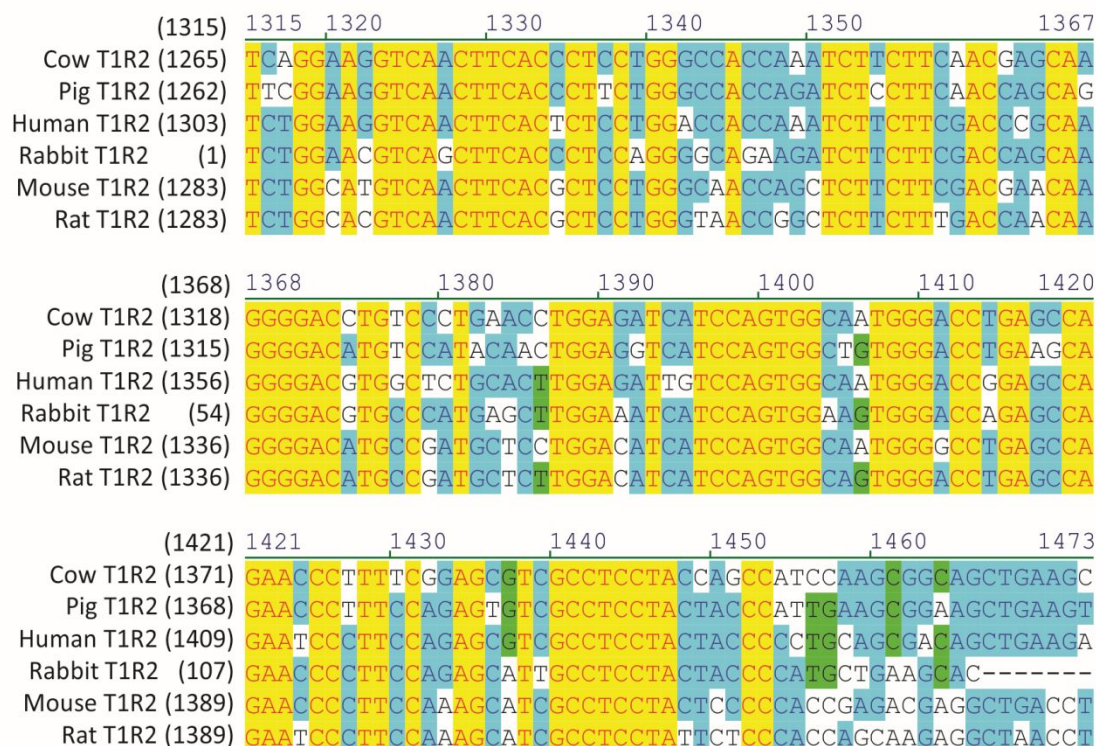
702

703

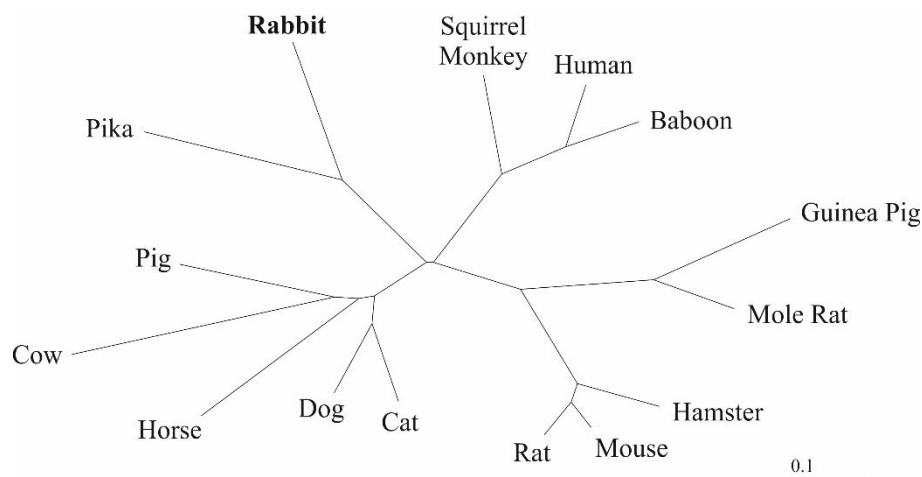
704 **Figure 5**

705

706

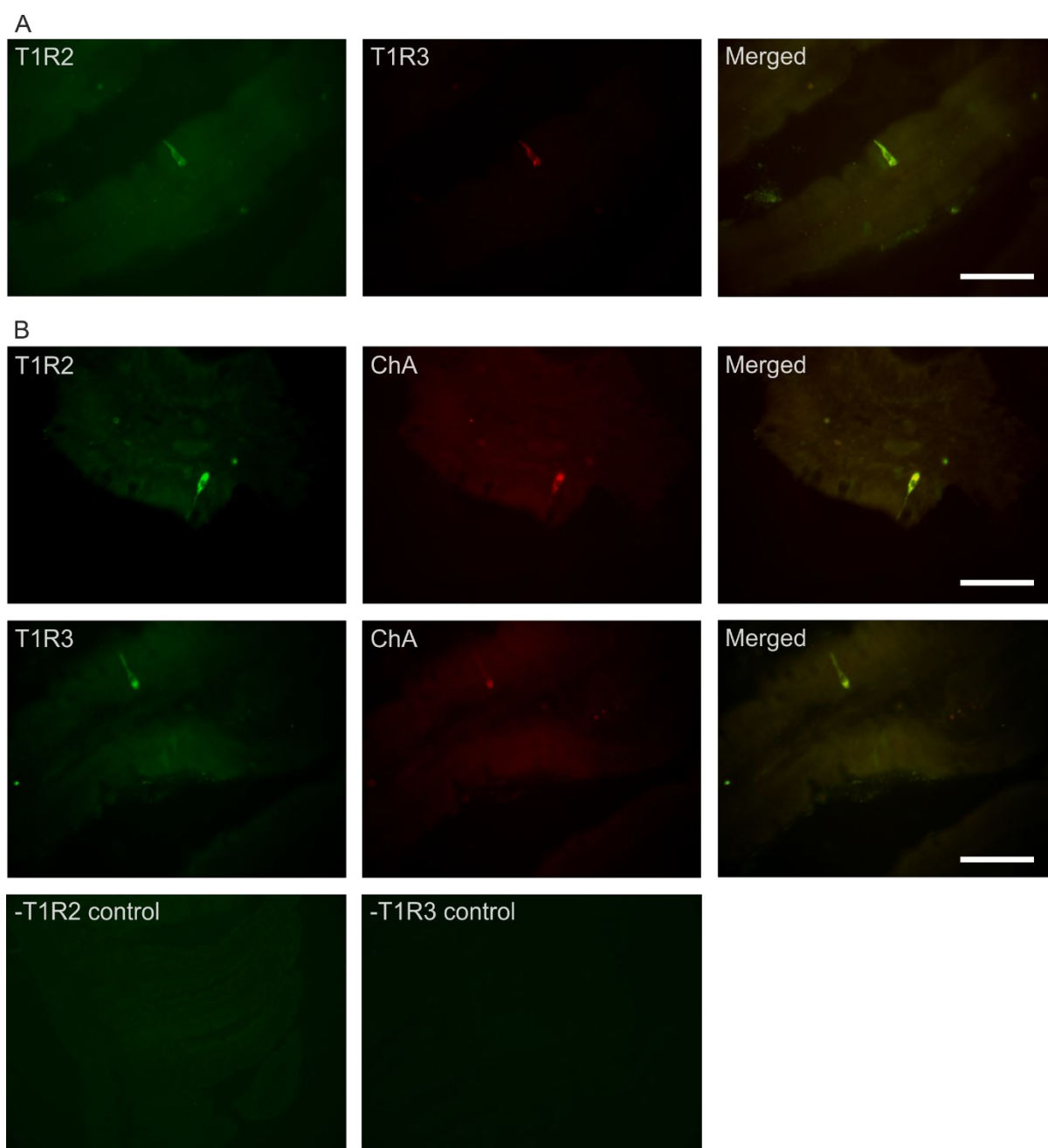
707 **Figure 6**

708

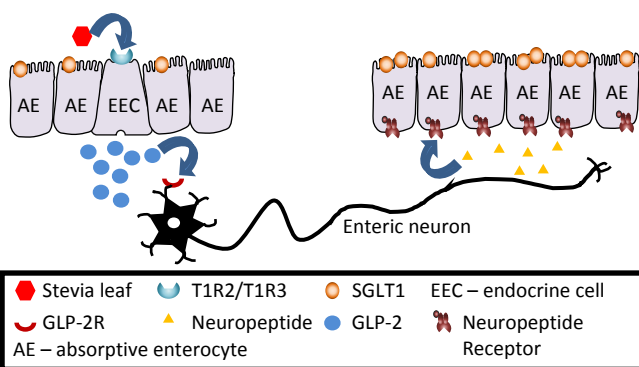
709 **Figure 7**

710

711

712 **Figure 8**

715 TOC



716